

MATERIAL QUALIFICATION OF LCLS-II PRODUCTION NIOBIUM MATERIAL INCLUDING RF AND FLUX EXPULSION MEASUREMENTS ON SINGLE CELL CAVITIES*

A. D. Palczewski[#], F. Marhauser,

Thomas Jefferson National Accelerator Facility, Newport News, VA, USA

A. Grassellino, S. Posen, Fermi National Accelerator Laboratory, Batavia, IL, USA

Abstract

It has been shown that cooldown details through transition temperature can significantly affect the amount of trapped magnetic flux in SRF cavities, which can lead to performance degradation proportional to the magnitude of the ambient magnetic field [1]. It has also more recently been shown that depending on the exact material properties - even when the material used originated from the same batch from the same vendor - and subsequent heat treatment, the percent of flux trapped during a cooldown could vary widely for identical cool-down parameters [2]. For LCLS-II, two material vendors have produced half of the niobium used for the cavity cells (Tokyo Denkai Co., Ltd. (TD) and Ningxia Orient Tantalum Industry Co., Ltd. (NX)). Both vendors delivered material well within specifications set out by the project (according to ASTM B 393-05), which allows yet some variation of material characteristics such as grain size and defect density. In this contribution, we present RF and magnetic flux expulsion measurements of four single cell cavities made out of two different niobium batches from each of the two LCLS-II material suppliers and draw conclusions on potential correlations of flux expulsion capability with material parameters. We present observations of limited flux expulsion in cavities made from the production material and treated with the baseline LCLS-II recipe.

INTRODUCTION

The LCLS-II prototype cavities currently being assembled into the first cryomodules were manufactured by Advanced Energy Systems, Inc. during the ILC R&D activity in the later 2000's out of material from ATI Wah Chang niobium. These cavities had little processing history and have eventually been treated with the now baseline LCLS-II recipe including bulk surface removal by Electropolishing (EP), heat treatment at 800°C for 3 hours and doping with nitrogen for 2 minutes, and finally a light 5-7 micron EP [3,4]. They all passed the current quality factor (Q_0) specification of 2.7×10^{10} at 16 MV/m with multiple cavities reaching 4.0×10^{10} through the use of superconducting flanges, careful environmental magnetic fields, and controlled cooldowns [5-8]. After welding the prototype cavities into the helium vessel, which has been carried out at FNAL, a small drop in the

average Q_0 has been experienced, but the average value was still above 3×10^{10} [8].

During the R&D phase, which aimed to develop a robust nitrogen-doping baseline recipe for LCLS-II to be applied by industrial cavity vendors, there were multiple advances in cavity treatment developed simultaneously, apart from the actual recipe development. First, it was shown that when residual magnetic fields are present, quickly cooling a cavity could significantly reduce the residual resistance; depend on the temperature gradient rather than the speed of cooling [1]. Soon after, the sensitivity of the surface resistance due to trapped flux was determined for nitrogen-doped cavities, which revealed a higher value ($n\Omega/mG$) compared to other treatments such as applying EP with 120°C bake as a result of the dependence on the surface mean free path [9-11]. Finally, it was shown that there is a very strong material dependence of the flux expulsion efficiency independent of surface preparation, RRR or material hardness, however a correlation was observed with annealing time and temperature, which also deviated among material from different suppliers. The combination of the above effects was most likely the cause of the wide performance variations in single-cell nitrogen-doping results carried out at JLab in 2014 during the initial LCLS-II R&D [5,6].

Because the treatment history and/or material of the cavities utilized for LCLS-II prototype cryomodules is different compared to production cavities, a clear understanding of the flux expulsion efficiency using the actual recipe with actual production material is needed. In this study, we present the RF and flux expulsion results from four single-cell cavities made from LCLS-II production material (TD, NX) applying the baseline recipe. We show that the LCLS-II material exhibits a wide range of flux expulsion efficiencies depending on the material origin/supplier and batches, but all material trap flux at levels, which would not allow to meet a specification of $Q_0 = 2.7 \times 10^{10}$ at 16 MV/m in a 5 mG field needed for the project, when applying the original baseline recipe.

LCLS-II MATERIAL

Niobium material being used for LCLS-II production cavities has been thoroughly inspected including Eddy-current scans at DESY (100% of half-cell sheets) resulting in a rejection rate of less than 2% and thus overall with a higher acceptance rate than for the XFEL high-end production for the same vendors (TD, NX). The

* Funding Agency: Authored by Jefferson Science Associates, LLC under U.S. DOE Contract No. DE-AC05-06OR23177.

[#] ari@jlab.org

Table 1: LCLS-II Material Used for Single Cell Studies

OTIC INGOT	RRR	HV Min	HV MAX	grain size ASTM	Cavity
ENT-132	380/412	44.6/35.7	56.6/39.3	5.5-6.0/5.0-5.5	RDTNX-01
ENT- 134	315/301	50.8/37.6	58.4/43.2	8.0/7.0-7.5	RDTNX-02
TD Ingot	RRR	HV Min	HV MAX	grain size ASTM	
1991	468	39.2	49.8	5	RDTTD-01
2022	365	36.4	42.5	7	RDTTD-02

quality control followed was almost identical to the XFEL quality checks as outlined by Brinkmann, *et al.* in 2010 and 2013 [12,13]. Following inspection, the sheets were and shipped to the cavity vendors Ettore Zanon S.p.A. and RI Research Instruments GmbH for cavity fabrication [14]. The niobium specification for LCLS-II is identical to the XFEL specifications. The project ordered 5720 half-cell sheets, which reserves material for cavities beyond those required for the 33 production cryomodules per LCLS-II baseline design (not accounting for the two prototype cryomodules) [3]. To produce this amount of sheets, both suppliers needed to produce multiple ingots with multiple heat treatment lots. Previous studies indicated a possible correlation between flux expulsion and enhanced grain size after annealing as well as the base RRR [2]. The two, RRR and grain size, are rather tightly correlated. Note that for cavity production, TD and NX material is not allowed to be mixed together in a single nine-cell cavity, but a cavity may contain niobium from different lots/ingots from a single material vendor.

The main material properties of the half-cell sheets chosen for the single-cell cavities are listed in Table 1. These comprise batches from TD and NX with high RRR/smallest grain and lowest RRR/largest grains. Because both material suppliers readily met the interstitial and contaminant elemental specifications, only the RRR, hardness and grain size specifications are shown (data are as provided by the vendors). The serial numbers chosen for the four single-cell cavities made from the four batches are shown in the last column.

FLUX EXPULSION SETUP AND DATA

To measure the flux expulsion efficiency, each cavity was cooled in a ~ 10 mG field from multiple base temperatures and with different helium flow rates similar to Posen, *et al.* [2]. The only differences between data taken at FNAL and JLab is the location of the temperature sensors and whether the ambient fields are controlled through the use of individual coils around the cavity (FNAL) or compensation coils located outside the Dewar (JLab). Figure 1 shows a picture of the JLab setup. Instead of having a single temperature sensor on the equator (FNAL), two sensors were located ~ 40 mm apart above and below the equator to provide a clearer measurement of the thermal gradient $\Delta T/cm$ at the equator during the cooldown. An example of a cooldown measurement is shown in Fig. 2. Each data point on the flux expulsion ratio curve is extracted from a graph like

this. The flux expulsions ratio is defined at the magnetic field after T_c divided by the magnetic field before T_c .

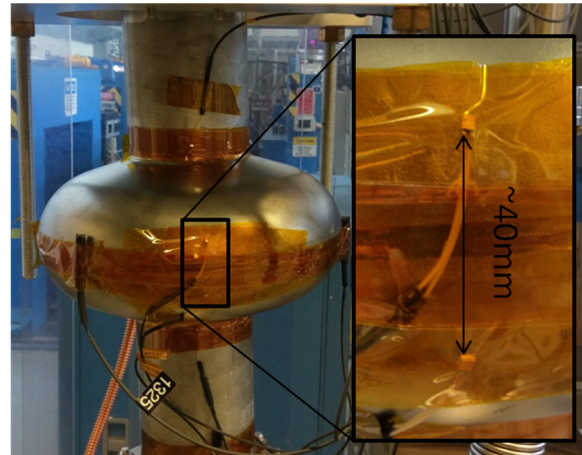


Figure 1: Flux expulsion measurement setup: three fluxgate magnetometers on the equator (120 degrees apart), 2 Cernox sensors, one on each iris and then 2 40 mm apart about the equator for local cooling rate.

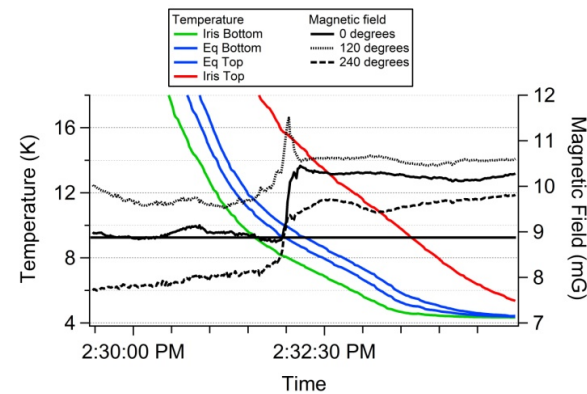


Figure 2: Example of flux expulsion ratio data from RDTTD-01 cooling from room temperature. Output: expulsion ratio of 1.15 for $\Delta T/cm = 0.18$ or iris to iris temperature of 7.2 K.

The flux expulsion data for the four single cell cavities is shown in Fig. 3. Both measurements are shown; Expulsion ratio vs. iris-to-iris temperature and vs. temperature gradient. The points encircled denote a test after a second nitrogen-doping was applied for the same cavity. Particularly, there was qualitatively no change in the flux expulsion efficiency after a second 800°C heat treatment, though the full data set was not recorded as in case of the first test series.

As a check for setup consistency and verification of the data prior to a retreatment with modified recipe, RDTTD-02 and RDTNX-02 were retested at FNAL. The corresponding iris-to-iris data are presented with open symbols in Fig. 3. Qualitatively, the two setups show the same results, but there is a difference below ~ 5 K. To compare with the previous LCLS-II data, we also show data from RDT-9 (a single cell cavity made from a material batch that yielded the highest average Q_0 at JLab during the LCLS-II prototype recipe development).

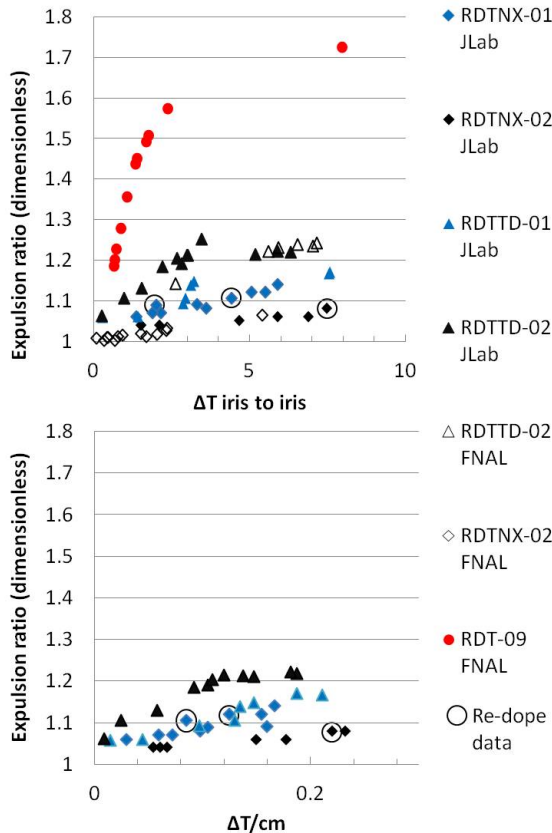


Figure 3: Flux expulsion ratio data iris-to-iris (top) and $\Delta T/cm$ (bottom); for comparison, data from a more ideal cavity RDT-9 non-LCLS-II production material in red circles. Circles data points are after additional EP/doping.

RF DATA

After the flux expulsion measurements were complete, each cavity was RF-tested in a low magnetic field environment ~ 1 mG and a high field ~ 5 mG, respectively, with a cooldown, which produces a 5 deg. C difference from iris to iris. The data is shown in Fig. 4. All cavities had specific issues during manufacturing, but are considered to not impact the outcome concerning the increase of the residual resistance as a function of the ambient magnetic field. The Q_0 vs. E_{acc} data plotted is for the cavities receiving 100 microns (TD cavities) and 200 microns (NX cavities) during the bulk EP. In order to understand the added residual resistance as a cause of trapped flux, we utilized the total residual resistance change divided by the change in ambient field and then

scaled it to the trapped flux for the given cooldown (see Table 2). All cavities except RDTNX-01 produced an added resistance of $n\Omega/mG \sim 0.9$ at 16 MV/m, consistent with other studies for the same doping recipe [15]. The data derived for RDTNX-01 was at 8 MV/m only since that cavity had a cateye defect, which pre-heated at very low field (~ 4 MV/m) and thus complicate the data analysis, though the finding does not deviate much from the published data (i.e. $n\Omega/mG \sim 0.75$ at 5 MV/m) [15]. With a BCS resistance of 5.5 n Ω at 16 MV/m plus a fundamental R_s of ~ 2 n Ω and an additional resistance of 3-5 n Ω due to trapped flux depending on the cooling, the material supplied for LCLS-II cavity production cannot yield cavities anymore complying to the original performance specification of $Q_0 = 2.7 \times 10^{10}$ at 16 MV/m (10 n Ω total) when the ambient field in the cryomodule is 5 mG.

Table 2: Calculated RF Losses and Trapped Flux Loss Ratio Extracted From the Expulsion Ratio and RF Data

Cavity	$R_s \Delta @ 16$ MV/m (n Ω)	Added Trapped flux scaled w/ ratio	$n\Omega/mG$ calculated with cooling rate flux ratio data
RDTTD-01	2.6	2.7	0.95
RDTTD-02	3.2	3.5	0.9
RDTNX-01	2.1#	3.6#	0.6#
RDTNX-02	3.6	3.8	0.93
# data @ 8MV/m			

These studies will be presented elsewhere. After positive results, the 900 deg. C heat treatment has now been implemented for the LCLS-II production cavities. An increase in the flux expulsion ratio is expected to a level where a magnetic of 5 mG will produce less than 2 n Ω of residual resistance. EP removal studies along with the 900°C annealing are also under investigation to understand why the cavities made from NX showed a lower fundamental R_s than the cavities made from TD, which had half the EP removal.

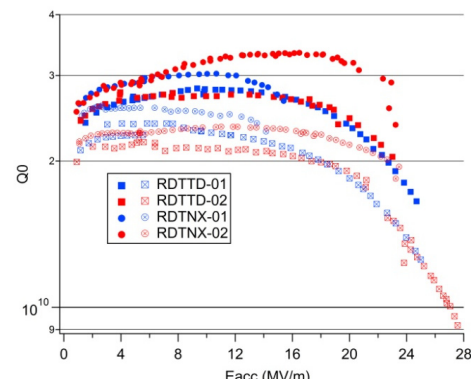


Figure 4: RF data for all 4 cavities in low field ~ 1 mG filled symbols and high magnetic field ~ 5 mG crossed open symbols. RDTNX-01/02 data is after a second round of doping/EP. Extracted residual resistance changes at 16 MV/m are summarized in Table 2.

REFERENCES

- [1] A. Romanenko, A. Grassellino, O. Melnychuk and D. A. Sergatskov, *J. Appl. Phys.*, vol. 115, p. 184903, 2014.
- [2] S. Posen, M. Checchin, A. C. Crawford, A. Grassellino, M. Martinello, O. S. Melnychuk, A. Romanenko, D. A. Sergatskov, and Y. Trenikhina, *J. Appl. Phys.*, vol. 119, p. 213903, 2016.
- [3] J. Galayda, *et. al.*, “LCLS-II Final Design Draft,” SLAC, Menlo Park, California, USA, Rep. LCLSII-1.1-DR-0251-R01-1, 2014.
- [4] A. Grassellino, *et al.*, *Superconductor Science and Technology* 26, p.102001, 2013.
- [5] C. E. Reece, A. D. Palczewski, *JLAB Tech notes* JLAB-TN-15-008, 2014.
- [6] A. D. Palczewski, R. Geng, C. E. Reece, in *Proc. LINAC2014*, Geneva, Switzerland, 2014, p. 736.
- [7] A. D. Palczewski, G. Eremeev, R.L. Geng, and C.E. Reece, in *IPAC2015*, Richmond, Virginia, 2015, WEPWI019, p. 3528.
- [8] M. Liepe, A. D. Palczewski, C. E. Reece, and A. Grassellino, in *Proc. SRF2015*, Whistler, BC, Canada, 2015, MOPB033, p. 159.
- [9] D. Gonnella, J. Kaufman, and M. Liepe, 2015, <http://arxiv.org/pdf/1509.04127v2.pdf>
- [10] S. Aull, and J. Knobloch, 2015, <http://arxiv.org/pdf/1507.04105v1.pdf>
- [11] M. Martinello, M. Checchin, A. Grassellino, O. S. Melnychuk, A. Romanenko, D. A. Sergatskov, in *Proceedings of SRF2015*, Whistler, BC, Canada, 2015, MOPB014, p. 110.
- [12] A. Brinkmann, M. Lengkeit, X. Singer, W. Singer, in *Proceedings of Linear Accelerator Conference LINAC2010*, Tsukuba, Japan, 2010, p. 788.
- [13] A. Brinkmann, S. Arnold, A. Ermakov, J. Iversen, M. Lengkeit, A. Pörschmann, L. Schäfer, W. Singer, X.Singer, in *Proceedings of SRF2013*, Paris, France, 2013, p. 171.
- [14] F. Marhauser, E. Daly, J.A. Fitzpatrick, in *Proceedings of SRF2015*, Whistler, BC, Canada, 2015, TUPB003, p. 529.
- [15] M. Martinello, A. Grassellino, M. Checchin, A. Romanenko, O. Melnychuk, D. A. Sergatskov, S. Posen, and J. F. Zasadzinski, *Appl. Phys. Lett.*, vol. 109, p. 062601, 2016.